Physics of the Solid State, 2025, Vol. 67, No. 8

08,10

# Migration of Si atoms on W(100) in surface tungsten silicide formation

© E.V. Rut'kov, E.Yu. Afanas'eva, N.R. Gall

Ioffe Institute,
St. Petersburg, Russia

E-mail: rutkov@ms.ioffe.ru

Received July 17, 2025
Revised July 18, 2025
Accepted July 18, 2025

Surface diffusion of silicon atoms on the W(100) surface was studied using Auger electron spectroscopy and thermal desorption methods in a wide range of coverages and temperatures. It was shown that the activation energy of migration changes from $E_{\mathrm{m}} \geq 1.8\,\mathrm{eV}$ at low Si coverages to $E_{\mathrm{m}} \approx 0.5\,\mathrm{eV}$ under WSi surface silicide formation.

**Keywords:** surface diffusion, adsorption, dissolution, desorption.

DOI: 10.61011/PSS.2025.08.62272.200-25

## 1. Introduction

Adsorption of Si on tungsten surfaces was extensively studied [1–11]. However, the most studies were focused on a behavior of Si adatoms on the W(110) face [1–6]. Tsong and Casanova [1,2] have studied adsorption of the Si atoms on the surface W(110) using a field ion microscope, Sault and Goodman [5,6] have studied a silicon superlattice formed on the surface W(110) depending on the Si coverage, using temperature-programmed desorption, Auger electron spectroscopy and low-energy electron diffraction (LEED). Diffusion of silicon into a tungsten bulk was studied by an atomic-probe method [7]. Adsorption of Si on polycrystalline tungsten surfaces was also studied by a thermal desorption method [8]. Diffusion of silicon into the tungsten bulk, migration over the surface for three low-index faces W(100), (110) and (111) was studied in the paper [11] using a density functional theory.

The silicon coverage makes it possible to significantly change adsorption and catalyst properties of tungsten. Thus, adsorption of CO, hydrogen and benzol was studied at 120 K on the silicon-covered surfaces W(110) [6]. The CO coverage decreased from $\vartheta = 0.80$ in saturation on the pure surface W(110) to $\vartheta = 0.40$ with 0.30 monolayer (ML) of silicon and to $\vartheta = 0.21$ with 0.56 ML of silicon. Dissociation of hydrogen, CO and benzol was significantly suppressed by silicon adsorbed on the tungsten surface. When annealing the silicon layers to $T = 1050\,\mathrm{K}$, a growth of tungsten silicide was observed, that resulted in an increase of catalyst activity of the surface. The Si–W system is considered to be a promising one in a technology of future nuclear fusion reactor, where tungsten acts as a diverter, while silicon is considered to be an element that protects walls from erosion [12,13].

In our previous studies we have investigated interaction of silicon with the surface W(100) by methods of Auger electron spectroscopy and thermal desorption [9,10]. It was shown that formation of a monolayer coverage with the concentration of silicon adatoms $N = 1 \cdot 10^{15}\,\mathrm{cm}^{-2}$ (the WSi surface silicide) at the temperatures 1100–1400 K resulted in active dissolution of newly arriving Si atoms in the substrate, which almost did not dissolve in it at the lower coverages. We have also determined an activation energy of desorption of silicon, which strongly depended on the coverage, varying form 6.1 to 4.7 eV when the coverage increased from $\vartheta_{\mathrm{Si}} = 0.1$ to $\vartheta_{\mathrm{Si}} = 1.0$. It can be expected that migration characteristics of the adatoms will also strongly vary when the coverage is changed, in particular, when reaching the concentration that corresponds to the surface silicide. The present study is aimed at determining the migration energy characteristics of silicon on W(100) within the coverage interval from a submonolayer one to formation of surface tungsten silicide.

## 2. Experimental methodology

Surface migration was investigated in the present study by simultaneously using two methods: the Auger electron spectroscopy (AES) allowing the detection of silicon adsorbed on the surface, but not dissolved in the bulk, and a method of temperature-programmed desorption (TPD), which provides information about the total concentration of silicon in the system both on the surface of tungsten and in its bulk.

The measurements were performed in ultrahigh vacuum of about $1 \cdot 10^{-10}\,\mathrm{Torr}$; thermal desorption of Si from W was recorded by a time-of-flight mass-spectrometer described in the study [9]. The electron Auger spectra were measured using a high-resolution prism electron Auger spectrometer ($\Delta E/E \approx 0.1\,\%$) allowing measurements to be carried out at the high (up to 2500 K) temperatures of the sample [10]. The samples were textured tungsten ribbons measuring $0.01 \times 1 \times 30\,\mathrm{mm}$ with predominant exit of the (100) face to the surface, which were heated by direct current. The ribbons were purified from impurities by a standard procedure: in the oxygen atmosphere at the pressure of $\sim 10^{-5}$ Torr and the temperature of 1500 K and then in ultrahigh vacuum at $T = 2500$ K. Only Auger peaks of tungsten were recorded after such purification. A rolling texture was replaced by a recrystallization one and the (100) face appeared on the surface. According to the X-ray diffraction data, a face orientation degree was $\sim 99.5$ %. A surface work function was $e\varphi = 4.65$ eV, which corresponded to the facet (100) W, and the surface was homogeneous in the work function with accuracy of $\pm 0.05$ eV. The time of sample heating from 300 to 2000 K or its cooldown to 300 K was below 1 s. In the TPD method, the sample was linearly heated at the rate of 200 Ks$^{-1}$.

The temperature of the samples at $T > 1100$ K was measured using an optical micropyrometer, and by linear extrapolation of the temperature dependence on the ribbon filament current to the room temperature in the range of the lower temperatures.

Silicon was deposited onto W(100) from rods of the sizes $1 \times 1 \times 30$ mm that were arranged in parallel to the tungsten ribbon symmetrically at its both sides, thereby making it possible to apply the coverages both to a working and a back side of the sample directly in ultrahigh-vacuum conditions. The chamber included collector systems for measuring thermal emission currents at both sides of the ribbon, this made possible to compare fluxes of silicon atoms falling on the front and the back side of the ribbon by change in the work function on them. The silicon fluxes were absolutely calibrated by a quartz microbalance, which is based on a phenomenon of shift of the resonance frequency of the quartz vibrator in deposition of thin films of a foreign substance onto it. The measurement procedure was as follows: silicon was deposited on the W ribbon at some temperature $T_W = \text{const}$ (on one side or both sides). Then the Si sputterers were switched off, the ribbon was cooled down to $T = 300$ K, which was followed by high-temperature flash or recording of the Auger spectra of silicon ($E_{Si} = 92$ eV) and tungsten ($E = 163{-}179$ eV). The intensity of the Auger signals was measured „peak-to-peak“. An amount of desorbed silicon was determined by an area of thermal desorption spectra on the mass number 28.

Deposition of silicon on both sides of the ribbon (the front and the back side, Figure 1, the insert) simplified correct interpretation of the experimental results.

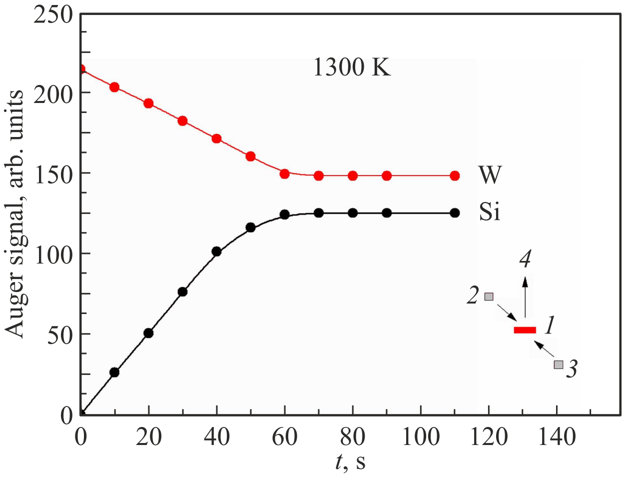

**Figure 1.** Variation of intensity of the Auger signals of silicon and tungsten on time when depositing the Si atoms to the W tape at both the sides when $T = 1300$ K. The density of the silicon flux was $\vartheta_{Si} \approx 1.7 \cdot 10^{13}$ cm$^2 \cdot$ s$^{-1}$. The insert includes a scheme of arrangement of the sputterers and the sample in the analytical chamber: *1* — the silicon sputterers; *2, 3* — the silicon sputterers; *4* — the inlet of the AES analyzer or the mass-spectrometer.

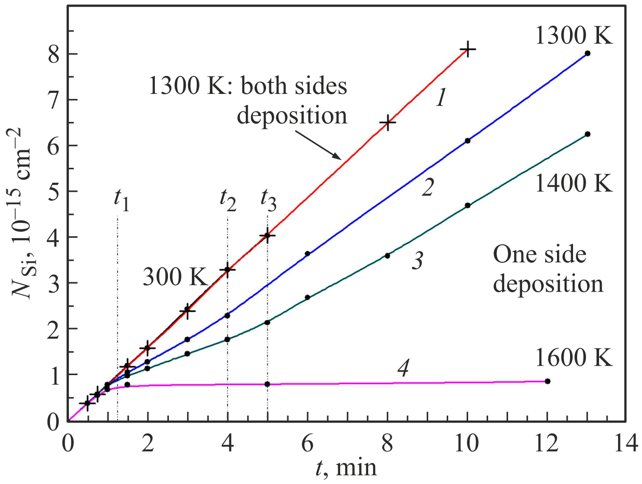

**Figure 2.** Dependences of the number of the desorbed silicon atoms on time of deposition at the various tungsten temperatures by the constant flux $\vartheta_{Si} \approx 1.3 \cdot 10^{13}$ cm$^{-2} \cdot$ s$^{-1}$. The curve *1* — both sides deposition at 300 and 1300 K; *2, 3, 4* — front-side deposition at 1300, 1400 and 1600 K, respectively.

## 3. Experimental results and discussion

Figure 1 shows a dependence of intensity of the Auger signals of silicon and tungsten on the silicon deposition time at $T = 1300$ K on both the sides of the ribbon with equal fluxes. It is clear that up to $t \approx 50$ s there is the linear dependence of increase of intensity of the Auger signal of silicon on time, wherein the concentration of silicon $N_{Si} = \upsilon_{Si} t$. Reaching a plateau on the graph corresponds to formation of the WSi surface compound (SC) with the concentration of the silicon atoms, equal to the monolayer $N_{Si} = 1 \cdot 10^{15}$ cm$^{-2}$ [10].

When $t > 60$ s, no accumulation of arriving silicon above $N_{Si} = 1 \cdot 10^{15}$ cm$^{-2}$ is observed on the surface, and, consequently, the silicon atoms are either desorbed or dissolved in the substrate bulk, or both the processes occur.

These questions can be answered by the TPD method.

Figure 2 shows the dependences of the amount of silicon detected by temperature-programmed desorption method on time of its deposition on the tungsten surface. The graph *1* that corresponds to deposition of silicon on both ribbon sides with the equal fluxes at $T = 1300\,\mathrm{K}$, is approximated by a straight line and coincides with the similar dependence obtained by deposition at $T = 300\,\mathrm{K}$. This supports an assumption of absence of noticeable thermal desorption of silicon at $T \leq 1300\,\mathrm{K}$. Consequently, after reaching the surface concentration $N_{\mathrm{Si}} = 1 \cdot 10^{15}\,\mathrm{cm}^{-2}$ (formation of the WSi SC) the whole deposited silicon is dissolved in the metal bulk. It results in a continuous increase in the area of the thermal desorption spectra with unchanged surface coverage, which is confirmed by the AES method (Figure 1).

When depositing silicon only on the front side of the ribbon at the same temperature $T = 1300\,\mathrm{K}$ (the curve *2*, Figure 2), it is clear that within the time range $0 < t < t_1$ the dependences *1* and *2* coincide — the WSi SC is formed on the surface. When $t > t_1$, there is a deviation of the curve *2* from the curve *1*. Since no desorption of Si from W is observed at this temperature, this fact of „loss“ of silicon can be explained only by migration of the silicon atoms to the back side of the ribbon. At the higher temperatures, one can expect „loss“ of silicon during its deposition on the front side of the ribbon not only due to migration to the back side, but due to desorption of the Si atoms from the surface as well (the curves *3* and *4* in Figure 2). In order to separate these two processes, silicon was deposited with the equal fluxes on both the sides of the ribbon, which allowed the migration fluxes to be balanced.

Figure 3 shows graphs of the dependences of the number of the desorbed silicon atoms on time of its deposition at the various temperatures of the substrate [9]. It is clear that when $T = 1400\,\mathrm{K}$ (the curve *2*) there is a deviation of the dependence of the amount of recorded silicon $N_{\mathrm{Si}}(t)$ from the linear one $N_{\mathrm{Si}} = \upsilon_{\mathrm{Si}} t$ (for 1300 K), which can be explained only by thermal desorption of the silicon atoms during deposition. It is obvious that the higher the temperature of the sample, the more effective desorption and the less silicon accumulated in the system (compare the dependences *1*–*4*, Figure 3).

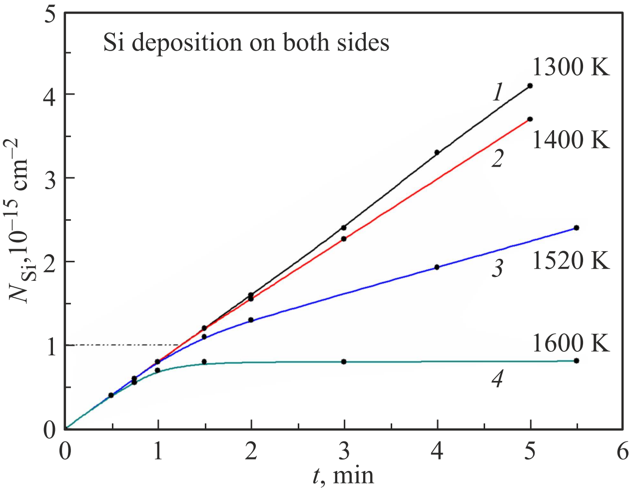

**Figure 3.** Dependences of the number of the desorbed silicon atoms on time of deposition on both the sides with the equal fluxes $\vartheta_{\mathrm{Si}} \approx 1.3 \cdot 10^{13}\,\mathrm{cm}^{-2} \cdot \mathrm{s}^{-1}$ at the various temperatures of tungsten $T$, K: the curve *1* — 1300, *2* — 1400, *3* — 1520, *4* — 1600.

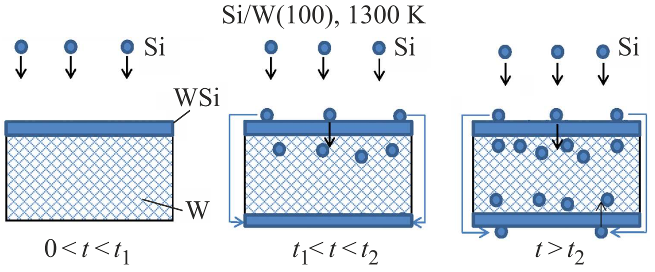

**Figure 4.** Schematic representation of the processes that occur in deposition of the silicon atoms only on the front side at $T = 1300\,\mathrm{K}$.

We note that during deposition of Si on the W ribbon at $T = 1600\,\mathrm{K}$, the concentration of the silicon atoms on the surface does not exceed $N_{\mathrm{Si}} = 0.8 \cdot 10^{15}\,\mathrm{cm}^{-2}$. The same results are provided by the AES method. At the same time, in case of deposition on the front side (the curve *4*, Figure 1) and on both the sides (the curve *4*, Figure 3) the dependences $N_{\mathrm{Si}}(t)$ almost coincide. It seems to be related to the fact that the desorption flux at such temperatures and surface silicon coverages significantly exceeds the migration flux and the flux of dissolution of the silicon atoms into the tungsten bulk.

A simplified physical picture of the processes on the surface W(100) in deposition of the silicon atoms is shown in Figure 4 (for clarity, geometrical sizes of the ribbon with a section of $10^{-2} \times 1\,\mathrm{mm}$ are highly distorted).

The dependence $N_{\mathrm{Si}}(t)$ (the curve *2*) in Figure 2, which is taken when $T = 1300\,\mathrm{K}$, has tow inflection points that correspond to times of deposition $t_1$ and $t_2$. Three sections can be distinguished on it: the first one, at $0 < t < t_1$, corresponds to a linear increase of the concentration of silicon on the surface to $N_{\mathrm{Si}} = 1 \cdot 10^{15}\,\mathrm{cm}^{-2}$ (formation of the WSi surface compound, Figure 4). Its formation is followed by a simultaneous start of active dissolution of the silicon atoms in tungsten and of migration of the Si atoms to the back side. The second section, at $t_1 < t < t_2$, exhibits Si migration to the back side of the ribbon and increase of the silicon coverage there to $N_{\mathrm{Si}} = 1 \cdot 10^{15}\,\mathrm{cm}^{-2}$ (formation of the surface silicide on the back side), Figure 4. After its formation, at $t > t_2$, silicon starts being actively dissolved in the substrate not only from the front side, but from the back side as well. After some time, a stationary mode is set. The concentration of the Si atoms along the entire surface of the W ribbon remains unchanged ($N_{\mathrm{Si}} \approx 1 \cdot 10^{15}\,\mathrm{cm}^{-2}$) and the rates of all the processes do not depend on time. Indeed, the points of the dependence *2* in the third section, $t > t_2$, fit well with the straight line (Figure 2). At the time of setting of the stationary mode, silicon in the concentration

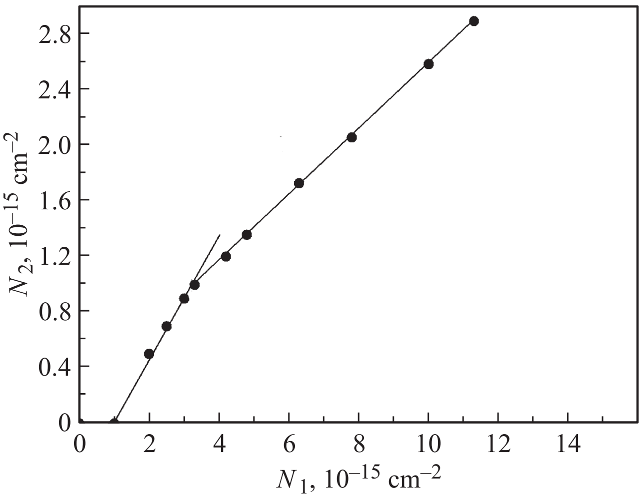

**Figure 5.** Dependence of Si loss due to migration to the back side of the ribbon $N_2$ on the number of the silicon atoms $N_1$ fallen on the front side at $T = 1300\,\mathrm{K}$; $\vartheta_{\mathrm{Si}} = 1.3 \cdot 10^{13}\,\mathrm{cm}^{-2} \cdot \mathrm{s}^{-1}$.

$N_{\mathrm{Si}} \approx 1 \cdot 10^{15}\,\mathrm{cm}^{-2}$ migrated to the back side of the ribbon at $T = 1300\,\mathrm{K}$, which corresponds to the proposed model. One should note a similar behavior of the dependence $N_{\mathrm{Si}}(t)$ taken at $T = 1400\,\mathrm{K}$ (Figure 2, the graph *3*) — the linear increase of the concentration to $N_{\mathrm{Si}} = 1 \cdot 10^{15}\,\mathrm{cm}^{-2}$, two inflection points at $t_1$ and $t_3$ with subsequent linear increase of the concentration of silicon (the stationary mode). In this case, all the above-described processes are somewhat long in time as compared to $T = 1300\,\mathrm{K}$, which is related to beginning thermal desorption of silicon (Figure 3), which results in loss of a part of the substance.

We reconstruct the graphs *1* and *2* (Figure 2) for $T = 1300\,\mathrm{K}$ in the following coordinates: the abscissa axis includes the total number of the silicon atoms that arrived on the front surface of the sample $N_1$ (in units of $\mathrm{cm}^{-2}$), and the ordinate axis includes the number of the atoms transferred to the back side of the ribbon $N_2$, in units of $\mathrm{cm}^{-2}$ as well (Figure 5). It is clear that first all the adatoms remain on the front surface and when approaching the concentration of silicon $N_{\mathrm{Si}} = 1 \cdot 10^{15}\,\mathrm{cm}^{-2}$ start migrating to the back side of the ribbon. When $N_1 \approx 3 \cdot 10^{15}\,\mathrm{cm}^{-2}$, silicon with $N_2 = 1 \cdot 10^{15}\,\mathrm{cm}^{-2}$ is transferred to the back side of the ribbon to form the surface silicide there as well. Then silicon in the concentration: $N_1 - 2N_2 = 1 \cdot 10^{15}\,\mathrm{cm}^{-2}$ diffused into the tungsten bulk from its front side. Thus, experience shows that the number of the silicon adatoms migrated to the back side of the ribbon is commensurable with the number of those dissolved in the tungsten bulk. This fact indirectly indicates that lifetimes of the Si adatoms relative to dissolution are similar to the times of migration of the atoms to the back side of the ribbon. These processes correspond to graph *2* in Figure 2 for the time $t_2 = 4\,\mathrm{min}$.

The experiment shows that after formation of the WSi SC, both on the front surface of the tungsten ribbon and its back side the migration processes actively continue — see Figure 2 (the curve *2* for $t > t_2$; the curve *3* for $t > t_3$) and Figure 5 for $N_1 > 3.2 \cdot 10^{15}\,\mathrm{cm}^{-2}$. Only a slope of the straight line is changed, which seems to be related to completion of formation of the WSi SC on the back side of the tape.

The average length $x$ of adatom migration in the direction perpendicular to a ribbon butt end over a certain time $t$ is determined by the formula $x = (2Dt)^{1/2}$ [14], in which $D = D_0 \exp[-E_{\mathrm{m}}/(k_{\mathrm{B}}T)]$ — the surface diffusion coefficient, $E_{\mathrm{m}}$ — the activation energy of migration over the tungsten surface, $k_{\mathrm{B}}$ — the Boltzmann constant. The value $D_0 = \lambda_0^2 k_{\mathrm{B}} T/h$, where $\lambda_0$ — the migration jump length [15]. If $\lambda_0 = 3\,\text{Å}$, then $D_0 \approx 2.7 \cdot 10^{-2}\,\mathrm{cm}^2 \cdot \mathrm{s}^{-1}$ at $T = 1300\,\mathrm{K}$. Thus,

$$x = 2D_0 t \exp[-E_{\mathrm{m}}/(k_{\mathrm{B}}T)]^{1/2}. \quad (1)$$

Let us evaluate the activation energy of migration for $\theta_{\mathrm{Si}} \geq 1$, using the AES method. For this purpose, silicon was additionally adsorbed at $T = 300\,\mathrm{K}$ on the WSi surface silicide formed on the front side, to the concentration $N_{\mathrm{Si}} = 0.3 \cdot 10^{15}\,\mathrm{cm}^{-2}$ and the temperature was raised to $T = 1300\,\mathrm{K}$. As follows from Figure 2, after formation of the surface silicide on the W surface, processes of dissolution and migration begin at $T = 1300\,\mathrm{K}$, wherein the fluxes of these processes are commensurable. The AES method has shown that „extra“ silicon leaves the front surface due to dissolution and migration for the time $t \approx 5\,\mathrm{s}$.

Thus, when $T = 1300\,\mathrm{K}$ the Si adatoms migrate over the WSi surface silicide (from the front side of the ribbon to the back side) for the time $t \approx 5\,\mathrm{s}$, passing the distance $x$ that is equal to a half of the ribbon width $l/2 = 0.05\,\mathrm{cm}$. Then it is possible to find that $E_{\mathrm{m}} \approx 0.5 \pm 0.1\,\mathrm{eV}$ from the formula (1).

This magnitude is close to a value calculated in the study [11] using the density functional method for migration of the silicon atoms in the second layer on the facet W(100): $E_{\mathrm{m}} = 0.62\,\mathrm{eV}$.

We have evaluated the activation energy of Si migration over the surface W(100) $E_{\mathrm{m}} \approx 0.5\,\mathrm{eV}$, when $\vartheta \geq 1$. Migration of silicon to the back side of the ribbon for the coverages $\vartheta < 1$ was not observed by us at any temperatures. Nevertheless, a lower limit of the activation energy of Si migration over the surface W(100) for these coverages can be evaluated from tests of desorption of Si from W using the AES method. Figure 6 shows, as an example, the desorption curve of silicon from tungsten with the initial state $\vartheta_{\mathrm{Si}} = 1$ at $T = 1835\,\mathrm{K}$, where the intensities of the Auger signal of silicon are recalculated into the degree of coverage. It is clear that when reaching a plateau $\vartheta_{\mathrm{Si}} = 0.38$, neither desorption, nor dissolution, nor migration of silicon to the back side of the ribbon is observed for 1 min ($\vartheta_{\mathrm{Si}} = \mathrm{const}$). Let us set a parameter $x$, which is a length of migration of the Si adatom for the test time of 60 s. Experimentally, it is easy to note possible losses of silicon due to migration of the adatoms in the amount of 10% (taking into account the two butt ends of the ribbon). It means that in our

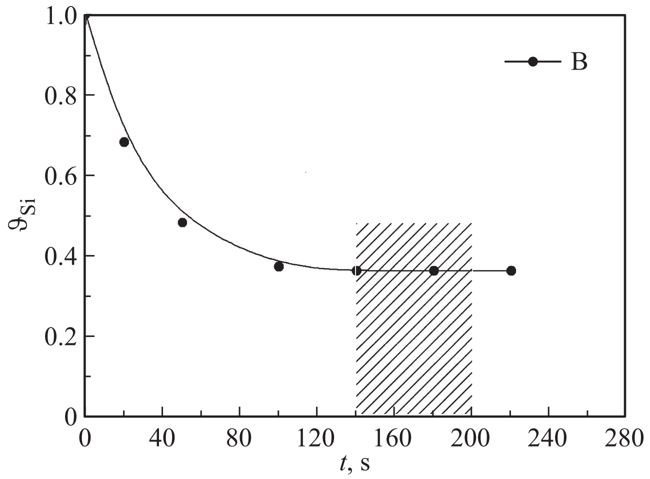

**Figure 6.** Dependence of silicon coverage on tungsten $\vartheta_{Si}$ on the ribbon annealing time at $T = 1835$ K. $\vartheta_{Si} = 1$ corresponds to the WSi SC when $N_{Si} = 1 \cdot 10^{15}$ cm$^{-2}$.

Dependence of the activation energy of surface migration of the silicon atoms on the coverage. The estimates were done by the results obtained at the temperatures specified in the second column of the table

| $\vartheta_{Si}$ | $T$, K | $E_m$, eV |
|---|---|---|
| $> 1$ | 1300 | 0.5 |
| 0.56 | 1600 | $\geq 1.5$ |
| 0.44 | 1700 | $\geq 1.6$ |
| 0.38 | 1765 | $\geq 1.65$ |
| 0.30 | 1835 | $\geq 1.7$ |
| 0.16 | 1900 | $\geq 1.75$ |
| 0.05 | 1965 | $\geq 1.81$ |

example $x \leq 5 \cdot 10^{-3}$ cm (the length of migration through one butt end of the ribbon). In this case, by substituting the values $t = 60$ s; $D_0 = 10^{-2}$ cm$^2 \cdot$ s$^{-1}$; $T = 1835$ K, it is possible to find by the formula (1) that $E_m \geq 1.7$ eV. The experience shows that the higher the annealing temperature, the smaller coverage of silicon corresponding to the plateau. With a decrease of the coverage, the activation energy of desorption and a dissolution activation energy increase and it is logical to expect that the activation energy of migration will increase, too.

The table shows a typical plateau temperature for certain coverage $\vartheta_{Si}$ and the estimate of the value $E_m$, which is calculated in the same way as in the above-considered example for $T = 1835$ K.

It is clear that $E_m$ when $\vartheta_{Si} < 1$ is significantly higher than for the coverages $\vartheta_{Si} > 1$. It is related to the fact that all the strongly-bound centers are already occupied by the silicon adatoms and further migration is essentially migration of silicon over the WSi surface silicide. It should be noted that the obtained estimates agree with values of the energy of activation of migration of the Si atoms on W(100), which are calculated by the density functional method: $E_m = 1.94$ eV when $\vartheta_{Si} \ll 1$ and $E_m = 0.62$ eV when $\vartheta_{Si} > 1$ [11].

An abrupt decrease of the activation energy of silicon migration in the second layer after formation of the surface silicide to $E_m \approx 0.5$ eV seems quite reasonable and fit well into general energetics of the processes on the surface W(100) with involvement of the silicon atoms. Indeed, after formation of the WSi SC ($\vartheta_{Si} = 1$) the activation energy of desorption of the silicon adatom from tungsten decreases from 6.1 eV at $\vartheta_{Si} \ll 1$ to 4.7 eV [9]. At low coverages, silicon is not dissolved in the tungsten bulk even at the temperatures 1800–1900 K, whereas after formation of the WSi SC the newly arriving Si atoms are quickly dissolved already at $T = 1100$ K [10].

## 4. Conclusion

It is shown that the value of the activation energy of silicon atoms migration over the tungsten surface significantly depends on the coverage and varies from the value$E_m > 1.8$ eV at the low submonolayer coverages to the value of about 0.5 eV under formation of the surface silicide. Qualitatively, similar changes in the energies of dissolution and desorption were also observed previously when approaching a state of the surface chemical compound for the various adsorption systems $M$–$X$, where $M$ — the metal substrate, and $X$ — the element of the group 3–6 of the Periodic table. Thus, for the system C–W (100) at the low coverages carbon started to dissolve in the metal bulk at $T \geq 1900$ K, but after formation of the WC surface carbide ($N_C = 1 \cdot 10^{15}$ cm$^{-2}$) the dissolution temperature decreased to 700–800 K. It seems that reaching this saturated adsorption state similarly affects the activation energy of migration and the similar behavior can be expected for the other adsorption systems as well.

### Conflict of interest

The authors declare that they have no conflict of interest.

## References

[1] R. Casanova, T.T. Tsong. Surf. Sci. **109**, *1*, L497 (1981). https://doi.org/10.1016/0039-6028(81)90505-7
[2] R. Casanova, T.T. Tsong. Thin Solid Films **93**, *1–2*, 41 (1982). https://doi.org/10.1016/0040-6090(82)90090-6
[3] C.A. Kiwanga, R.A. Collins. Physica Status Solidi (a) **23**, *1*, 209 (1974). https://doi.org/10.1002/pssa.2210230122
[4] A.P. Janssen, J.P. Jones. Surf. Sci. **41**, *1*, 257 (1974). https://doi.org/10.1016/0039-6028(74)90308-2
[5] A.G. Sault, D.W. Goodman. Surf. Sci. **235**, *1*, 28 (1990). https://doi.org/10.1016/0039-6028(90)90103-F
[6] A.G. Sault, D.W. Goodman. J. Catal. **126**, *1*, 57 (1990). https://doi.org/10.1016/0021-9517(90)90046-M

[7] O. Nishikawa, Y. Tsunachima, E. Nomura, S. Horie, M. Wada, M. Shibata, T. Yoshimura, R. Uemori. J. Vac. Sci. Technol. B **1**, *1*, 6 (1983). https://doi.org/10.1116/1.582506

[8] M. Hashimoto, T. Matsushima, K. Azuma, T. Matsui. Surf. Sci. **137**, *1*, L75 (1984). https://doi.org/10.1016/0039-6028(84)90671-X

[9] V.N. Ageev, E.Yu. Afanas'eva. Poverkhnost' **7**, 30 (1987). (in Russian).

[10] V.N. Ageev, E.Yu. Afanas'eva, N.R. Gall', S.N. Mikhailov, E.V. Rut'kov, A.Ya. Tontegode. Poverkhnost', **5**, 6 (1987). (in Russian).

[11] L. Yang, B.D. Wirth. Nucl. Fusion **63**, *12*, 126004 (2023). https://doi.org/10.1088/1741-4326/acf4a9

[12] Z.L. Tang, G.Z. Zuo, C.L. Li, M. Huang, X.B. Zhang, J.S. Hu. J. Nucl. Mater. **555**, 153146 (2021). https://doi.org/10.1016/j.jnucmat.2021.153146

[13] H. Mao, F. Ding, G.-N. Luo, Z. Hu, X. Chen, F. Xu, J. Hu, G. Zuo, Z. Sun, Y. Yu, J. Wu, L. Wang, Y. Duan, J. Xu, J. Chen, Z. Yang, R. Ding, H. Xie. Nucl. Mater. Energy **12**, 447 (2017). https://doi.org/10.1016/j.nme.2016.12.010

[14] T.T. Tsong. Rep. Prog. Phys. **51**, *6*, 759 (1988). https://doi.org/10.1088/0034-4885/51/6/001

[15] A.G. Naumovets, Yu.S. Vedula. Surf. Sci. Rep. **4**, *7–8*, 365 (1985). https://doi.org/10.1016/0167-5729(85)90007-X

*Translated by M.Shevelev*